

## RESEARCH ARTICLE

10.1002/2014GB004969

## Special Section:

Trends and Determinants of the Amazon Rainforests in a Changing World, A Carbon Cycle Perspective

## Key Points:

- Vertical atmospheric gradients of DMS characterized in the central Amazon
- Enclosure and atmospheric studies indicate both soil and vegetation sources
- Results suggest important climate impact(s) via aerosol and cloud processes

## Supporting Information:

- Text S1 and Figures S1–S6

## Correspondence to:

K. Jardine,  
kjardine@lbl.gov

## Citation:

Jardine, K., et al. (2015), Dimethyl sulfide in the Amazon rain forest, *Global Biogeochem. Cycles*, 29, 19–32, doi:10.1002/2014GB004969.

Received 15 AUG 2014

Accepted 4 DEC 2014

Accepted article online 8 DEC 2014

Published online 8 JAN 2015

Corrected 27 JUN 2016

The copyright line for this article was changed on 27 JUN 2016 after the original publication.

©2015. The Authors.

This is an open access article under the terms of the Creative Commons Attribution License, which permits use, distribution and reproduction in any medium, provided the original work is properly cited.

## Dimethyl sulfide in the Amazon rain forest

K. Jardine<sup>1</sup>, A. M. Yañez-Serrano<sup>2</sup>, J. Williams<sup>3</sup>, N. Kunert<sup>4</sup>, A. Jardine<sup>2</sup>, T. Taylor<sup>5</sup>, L. Abrell<sup>6</sup>, P. Artaxo<sup>7</sup>, A. Guenther<sup>8</sup>, C. N. Hewitt<sup>9</sup>, E. House<sup>9</sup>, A. P. Florentino<sup>2</sup>, A. Manzi<sup>2</sup>, N. Higuchi<sup>2</sup>, J. Kesselmeier<sup>3</sup>, T. Behrendt<sup>3</sup>, P. R. Veres<sup>3</sup>, B. Derstroff<sup>3</sup>, J. D. Fuentes<sup>10</sup>, S. T. Martin<sup>11</sup>, and M. O. Andreae<sup>3</sup>

<sup>1</sup>Climate Science Department, Earth Science Division, Lawrence Berkeley National Laboratory, Berkeley, California, USA, <sup>2</sup>National Institute for Amazon Research, Manaus, Brazil, <sup>3</sup>Atmospheric Chemistry and Biogeochemistry Departments, Max Planck Institute for Chemistry, Mainz, Germany, <sup>4</sup>Max Planck Institute for Biogeochemistry, Jena, Germany, <sup>5</sup>Department of Ecology and Evolutionary Biology, University of Arizona, Tucson, Arizona, USA, <sup>6</sup>Departments of Chemistry and Biochemistry and Soil, Water and Environmental Science, University of Arizona, Tucson, Arizona, USA, <sup>7</sup>Institute of Physics, University of São Paulo, São Paulo, Brazil, <sup>8</sup>Pacific Northwest National Laboratory, Richland, Washington, USA, <sup>9</sup>Lancaster Environment Centre, University of Lancaster, Lancaster, UK, <sup>10</sup>Department of Meteorology, College of Earth and Mineral Sciences, Pennsylvania State University, University Park, Pennsylvania, USA, <sup>11</sup>School of Engineering and Applied Sciences and Department of Earth and Planetary Sciences, Harvard University, Cambridge, Massachusetts, USA

**Abstract** Surface-to-atmosphere emissions of dimethyl sulfide (DMS) may impact global climate through the formation of gaseous sulfuric acid, which can yield secondary sulfate aerosols and contribute to new particle formation. While oceans are generally considered the dominant sources of DMS, a shortage of ecosystem observations prevents an accurate analysis of terrestrial DMS sources. Using mass spectrometry, we quantified ambient DMS mixing ratios within and above a primary rainforest ecosystem in the central Amazon Basin in real-time (2010–2011) and at high vertical resolution (2013–2014). Elevated but highly variable DMS mixing ratios were observed within the canopy, showing clear evidence of a net ecosystem source to the atmosphere during both day and night in both the dry and wet seasons. Periods of high DMS mixing ratios lasting up to 8 h (up to 160 parts per trillion (ppt)) often occurred within the canopy and near the surface during many evenings and nights. Daytime gradients showed mixing ratios (up to 80 ppt) peaking near the top of the canopy as well as near the ground following a rain event. The spatial and temporal distribution of DMS suggests that ambient levels and their potential climatic impacts are dominated by local soil and plant emissions. A soil source was confirmed by measurements of DMS emission fluxes from Amazon soils as a function of temperature and soil moisture. Furthermore, light- and temperature-dependent DMS emissions were measured from seven tropical tree species. Our study has important implications for understanding terrestrial DMS sources and their role in coupled land-atmosphere climate feedbacks.

## 1. Introduction

Volatile-reduced sulfur compounds are continuously exchanged between the atmosphere and the biosphere, with natural gas phase emission estimates of  $65 \pm 25$  teragrams of sulfur per year ( $\text{Tg S a}^{-1}$ ) and anthropogenic emissions of  $93 \pm 15 \text{ Tg S a}^{-1}$  [Andreae and Jaeschke, 1992]. Reduced sulfur species influence processes such as air pollution and acid rain via the production of sulfuric acid [Kanda and Tsuruta, 1995; Staubes et al., 1989; Zhigang et al., 2010], which is also considered the most important chemical component in new aerosol particle formation (NPF) [Kulmala et al., 2004; Sipilä et al., 2010]. Through the formation of secondary sulfate aerosols, which can act as potent cloud condensation nuclei (CCN), dimethyl sulfide (DMS,  $\text{CH}_3\text{SCH}_3$ ) emissions from marine phytoplankton were hypothesized to have a significant impact on global climate [Lovelock et al., 1972], giving rise to the hypothesis (Charlson, Lovelock, Andreae, and Warren (CLAW) hypothesis) of a strong biological control over climate through a feedback loop that operates between ocean ecosystems and the atmosphere [Charlson et al., 1987]. While other marine sources of CCN, such as organics and sea-salt aerosols, are potentially more important [Quinn and Bates, 2011], model simulations suggest that DMS emissions are nonetheless a significant driver of oceanic cloud formation, its properties, and precipitation patterns [Thomas et al., 2010]. Over the remote continents, e.g., Amazonia and central Siberia, secondary organic matter dominates the chemical composition of aerosols in the optically and cloud microphysically active size range [Chi et al., 2013; Pöschl et al., 2010]. However, the mechanisms leading to NPF in these regions are still unclear, and even relatively small amounts of gaseous sulfuric acid formed from the oxidation of DMS might be important through their role in facilitating NPF.

DMS emission measurements have been reported from soils and leaf litter [Kesselmeier and Hubert, 2002; Lamb et al., 1987; Staubes et al., 1989; Yang et al., 1996] with possible sources from the microbial metabolism of sulfur-containing amino acids [Banwart and Bremner, 1975; Zhang et al., 2004]. Although DMS emissions have also been reported from vegetation [Fall et al., 1988; Geng and Mu, 2006; Jardine et al., 2010a; Kanda and Tsuruta, 1995; Kesselmeier et al., 1993; Yonemura et al., 2005], ecosystem-scale observations remain extremely rare, leaving large uncertainties with regard to the potential importance of terrestrial DMS sources. While plant surveys revealed that most plants studied emit only small amounts of DMS to the atmosphere [Geng and Mu, 2006; Yonemura et al., 2005], large DMS emission rates that increased with light and temperature have been reported from a rainforest tree species in Cameroon [Kesselmeier et al., 1993], agricultural plants like corn [Fall et al., 1988], rice paddies [Zhigang et al., 2008], and the desert plant creosotebush [Jardine et al., 2010a]. Nonetheless, model simulations suggest that globally, terrestrial DMS sources are small (7% of total) compared to marine phytoplankton sources (85% of total) [Kettle and Andreae, 2000; Watts, 2000]. Although terrestrial biota are assumed to play a small role in the global cycling of DMS [Bingemer et al., 1992; Watts, 2000], only limited vertical gradient measurements of ambient DMS mixing ratios have been performed over tropical [Andreae and Andreae, 1988] and temperate forests [Berresheim and Vulcan, 1992]. However, previous studies measuring DMS mixing ratios in the lower troposphere by proton transfer reaction-mass spectrometry (PTR-MS) aboard an aircraft revealed higher DMS mixing ratios above a tropical rainforest in Surinam than over the ocean. Although the authors were not certain that the entire PTR-MS signal at  $m/z$  63 was from DMS, no other candidate compounds were considered plausible [Crutzen et al., 2000; Williams et al., 2001]. Although lower mixing ratios were observed, additional aircraft studies above the tropical forest of Guyana confirmed that the terrestrial boundary layer can be a source of DMS to the troposphere [Gregory et al., 1986].

In addition to plants, microbially produced DMS emissions have been reported from soils and leaf litter [Banwart and Bremner, 1975; Fall et al., 1988; Kesselmeier and Hubert, 2002; Staubes et al., 1989; Zhigang et al., 2010] and are triggered by higher water content and temperature [Staubes et al., 1989], which also stimulate soil respiration [Kesselmeier and Hubert, 2002]. DMS emissions have also been shown to be sensitive to pH [Zhang et al., 2004] and soil type [Lamb et al., 1987; Staubes et al., 1989]. Because DMS is poorly soluble in water (Henry's constant:  $0.4 \text{ mol kg}^{-1} \text{ bar}^{-1}$  at  $25^\circ\text{C}$ ) [Debruyen et al., 1995], it can be degassed rapidly as long as the soil is not saturated. Thus, the demonstrated dependence of DMS emissions from terrestrial ecosystem components (plants and soils) on temperature, light, and moisture suggests a potentially strong yet unexplored biota-chemistry-climate feedback mechanism. Terrestrial DMS emissions may play important roles in regional precipitation dynamics over land, especially in areas such as the Amazon Basin, which are remote from anthropogenic reduced sulfur gases and aerosol inputs [Barth et al., 2005]. Therefore, terrestrial DMS emissions could have important indirect effects on the global climate through the alteration of direct light into diffuse light that promotes enhanced forest-atmosphere exchange of  $\text{CO}_2$  [Gu et al., 1999] and water cycling linked to precipitation patterns. The Amazon Basin contains about half of the world's tropical rainforest [Myers, 1991] and processes each year more than twice the amount of anthropogenically emitted  $\text{CO}_2$  [Malhi and Grace, 2000; Phillips et al., 2009]. Atmospheric warming and changing precipitation patterns over the Basin are expected in the course of this century to result in large biophysical feedbacks to global  $\text{CO}_2$  climate forcing [Betts et al., 2004; Cox et al., 2008]. Thus, understanding the factors driving precipitation patterns in the Basin is of critical importance to the development of more accurate regional and global climate models [Malhi and Grace, 2000].

Here we examine light and temperature dependence of DMS emissions from leaves of several tropical plant species and soil moisture and temperature dependence of DMS emissions from Amazon soil. We also report the first chemical confirmation that DMS is present in the Amazon atmosphere and demonstrate that an ecosystem in the central Amazon Basin is a net source of this trace gas climatically important to the atmosphere. Our observations provide the first continuous real-time mixing ratio measurements of DMS vertical forest profiles in the Amazon Basin site over a 5 month period during 2010–2011 as well as high spatially resolved daytime vertical profiles during 2013–2014.

## 2. Methodology

### 2.1. DMS Identification and Quantification

Because DMS mixing ratios are expected to be in the low parts per trillion (ppt) range in ambient air [Andreae et al., 1990; Andreae and Andreae, 1988], highly sensitive and specific sensors are required in order to identify

and quantify DMS. A further challenge is to quantify temporal and vertical DMS mixing ratio patterns within and above forest canopies in order to evaluate potential DMS terrestrial sources. In this study, we utilized both quadrupole and time-of-flight proton transfer reaction-mass spectrometry (PTR-MS and PTR-TOF-MS) and offline gas chromatography-mass spectrometer (GC-MS) methods to quantify branch and soil DMS emissions as well as temporal and vertical ambient mixing ratio patterns in a natural primary rainforest in the central Amazon. We characterized the selectivity and sensitivity to DMS of each analytical system through an assessment of calibration intercomparisons using dynamic solution injection and compressed gas dilution. We also tested potential humidity dependencies and interferences from protonated acetaldehyde hydration and compared ambient mixing ratio measurements between GC-MS (K34 tower, 2013–2014) and PTR-MS (TT34 tower, 2010–2011). Finally, a comparison was made between these ambient DMS mixing ratio measurements and those from a 1980s study in the central Amazon (Reserve Ducke) [Andreae and Andreae, 1988].

## 2.2. Amazon Field Site

High temporally resolved DMS ambient mixing ratio measurements were carried out in the Amazon forest at the TT34 tower (2°35′40.20″S, 60°12′33.42″W; 107 m above sea level (asl)) between September 2010 and January 2011. In addition, high vertically resolved ambient mixing ratios were carried out at the nearby K34 walkup tower (2°35′48.09″S, 60°13′11.43″W; 110 m asl) between November 2013 and February 2014. The TT34 and K34 towers are located in the Reserva Biologica do Cueiras in central Amazonia, 60 km NNW of the city of Manaus, Brazil, and managed by INPA (Instituto Nacional de Pesquisas da Amazônia) under the Large-Scale Biosphere-Atmosphere Experiment in Amazonia program [Martin *et al.*, 2010a]. The vegetation in this area is considered to be undisturbed, mature, *terra firme* rainforest, with a leaf area index of 5–6 and an average canopy height of 30 m [Karl *et al.*, 2009].

## 2.3. Proton Transfer Reaction-Mass Spectrometry in the Amazon

Real-time ambient mixing ratios of DMS on the TT34 tower were quantified using a high-sensitivity proton transfer reaction-mass spectrometer (PTR-MS, Ionicon, Austria). The PTR-MS was operated under standard conditions with a drift tube voltage of 600 V and drift tube pressure of 2.0 hPa. Optimization of PTR-MS conditions resulted in high and sustained primary ion intensities ( $2\text{--}4 \times 10^7$  counts per second (cps)  $\text{H}_3\text{O}^+$ ) with low water cluster ( $\text{H}_2\text{O}\text{--}\text{H}_3\text{O}^+ < 4\% \text{H}_3\text{O}^+$ ) and low  $\text{O}_2^+$  ( $\text{O}_2^+ < 4\% \text{H}_3\text{O}^+$ ) formation. The following mass-to-charge ratios ( $m/z$ ) were sequentially monitored during each PTR-MS measurement cycle: 21 ( $\text{H}_3^{18}\text{O}^+$ ), 32 ( $\text{O}_2^+$ ), 37 ( $\text{H}_2\text{O}\text{--}\text{H}_3\text{O}^+$ ) with a dwell time of 20 ms each and 63 ( $\text{DMS}\text{--}\text{H}^+$ ) with a dwell time of 5 s. While adsorptive losses to surfaces during sampling are potentially a major issue for quantifying DMS in air samples, gas sampling line losses were minimized by regulating their temperature at 50°C using self-regulating heating tape (Omega Engineering, USA) in an insulated jacket. Raw signals (counts per second  $m/z$  63,  $\text{cps}_{63}$ ) were normalized by the adjusted primary ion signal ( $\text{cps}_{21}$ ) to obtain normalized counts per second ( $\text{ncps} = \text{cps}_{63}/\text{cps}_{21}$ ). The adjusted primary ion signal ( $\text{cps}_{21}$ ) was obtained by multiplying the signal at  $m/z$  21 ( $\text{H}_3^{18}\text{O}^+$ ) by the oxygen isotopic ratio of a representative natural abundance water sample ( $^{16}\text{O}/^{18}\text{O} = 500$ ).

Calibration slopes ( $\text{ppb ncps}^{-1}$ ) for DMS were obtained using the dynamic solution injection (DSI) technique [Jardine *et al.*, 2010b] which provided gas phase mixing ratios of 0–61 ppb and by dynamic dilution of a 500 ppb commercial compressed gas standard (Apel-Riemer, USA), which provided gas phase mixing ratios of 0.0–5.0 ppb. For the DSI technique, a 0.68 mM solution was prepared by diluting 5  $\mu\text{L}$  of an authentic DMS standard (99%, Sigma-Aldrich, USA) in 100 mL of cyclohexane. The solution was injected into the mixing vial at 0.0, 0.5, 1.0, 2.0, and 4.0  $\mu\text{L min}^{-1}$  (30 min each flow rate) with a constant dilution flow of 1.0  $\text{L min}^{-1}$  ultrahigh purity nitrogen. For both methods, calibration slopes were obtained by linear regression of the DMS mixing ratio versus the normalized PTR-MS signal ( $\text{ncps } m/z$  63). Sample air DMS mixing ratios were calculated by multiplying the sample normalized counts per second signal by the calibration slope after subtracting the background signal obtained in hydrocarbon-free air.

To investigate the possibility that the PTR-MS  $m/z$  63 signals may have arisen from protonated acetaldehyde-water clusters, we studied the effect of humidity and acetaldehyde mixing ratios on the PTR-MS signal at  $m/z$  63, which could be due to an acetaldehyde-water cluster ( $m/z$  45 + 18 = 63) instead of DMS. Zero air humidified with a dew point generator to a dew point of 20°C (LI610, Licor Biosciences, USA) was introduced into the PTR-MS while signals at  $m/z$  45 and  $m/z$  63 were measured. After establishing background signals,

a high mixing ratio (19 ppb) of acetaldehyde was added to the air sample to determine the potential for acetaldehyde-water cluster formation and interference on  $m/z$  63. The results demonstrate that the interference of acetaldehyde on  $m/z$  63 can be ignored (see section 3.1 for details).

#### 2.3.1. PTR-MS at the TT34 Tower

The PTR-MS gradient measurement scheme employed at the TT34 tower included six ambient air inlets extending throughout and above the 30 m tall canopy at heights of 2, 11, 17, 24, 30, and 40 m. The six inlets were sequentially analyzed for DMS mixing ratios (10 min at each inlet, one complete canopy profile per hour). In order to allow for equilibration of the sampling system after switching to the new sample trace gas mixing ratios at the next level, vertical gradients were calculated by averaging the last 7 min of each 10 min measurement period. The air sampling tubing lengths were equal to the inlet heights plus an additional 4 m each to reach the detector in the instrument container directly adjacent to the tower. Ambient air was drawn through each 0.64 cm outer diameter (O.D.) Teflon perfluoroalkoxy tube in parallel, using an oil-free diaphragm pump (KNF Neuberger, Germany) with a sample point to detector delay time of  $< 15$  s. Prior to each vertical gradient ambient air measurement period (lasting 4–7 days), ultrahigh purity nitrogen was run for 2 h directly into the PTR-MS to obtain instrument background signals. From this data, a DMS limit of detection of 8–12 ppt was estimated for the PTR-MS by multiplying the DSI calibration slope by twice the standard deviation of 7 min background signals.

#### 2.4. Gas Chromatography-Mass Spectrometry

Air samples were collected and analyzed for DMS using two similar thermal desorption-gas chromatography-mass spectrometry (TD-GC-MS) systems. In the tropical mesocosm biome in Arizona, USA, DMS was analyzed using a Series 2 air server connected to a Unity 2 thermal desorption system (MARKES International, UK) interfaced with a 5975C series gas chromatograph/electron impact mass spectrometer with a triple-axis detector (Agilent Technologies, USA). In Brazil (National Institute for Amazon Research, Manaus, Brazil), thermal desorption tube air samples from the Amazon field site were analyzed using a TD100 thermal desorption system (Markes International, UK) interfaced with a 5975C series gas chromatograph/electron impact mass spectrometer with a triple-axis detector (Agilent Technologies, USA).

##### 2.4.1. GC-MS Analysis at the K34 Tower

In the Amazon, high vertically resolved profiles of ambient DMS mixing ratios within and above the canopy were carried out at the K34 walkup tower using thermal desorption GC-MS. Samples were collected during the daytime (13:00–16:30) using a mechanical hand pump (EasyVOC, Markes International, UK) which drew 1.0 L of ambient air in approximately 4 min through conditioned stainless steel thermal desorption tubes fitted with internal SafeLok caps and packed with Tenax TA, Carbograph 1TD, and Carboxen 1003 sorbents. Each profile was completed within approximately 1 h and consisted of 13 measurement points (ground plus 12 platform levels, each with a 4.2 m vertical separation). Sample thermal desorption tubes were analyzed by thermal desorption GC-MS within 1 day following collection by dry purging for 10 min with  $20 \text{ mL min}^{-1}$  of helium carrier gas before being transferred to the cold trap held at  $20^\circ\text{C}$  (Air Toxics, Markes International, UK). Volatiles were desorbed by heating to  $300^\circ\text{C}$  for 10 min with  $20 \text{ mL min}^{-1}$  of carrier gas. During injection, the trap was heated to  $300^\circ\text{C}$  for 3.0 min while back flushing with carrier gas at a flow of  $3.5 \text{ mL min}^{-1}$  with  $2.0 \text{ mL min}^{-1}$  vented through the split and  $1.5 \text{ mL min}^{-1}$  directed to the column (Rtx 624 with intragard 60 m + 1 m guard  $\times 0.32 \text{ mm} \times 1.8 \mu\text{m}$ , Restek Inc., USA). Following sample injection, the GC oven was temperature programmed with an initial hold of 3 min at  $35^\circ\text{C}$  followed by an increase to  $230^\circ\text{C}$  at  $6^\circ\text{C min}^{-1}$ . The mass spectrometer was configured for trace analysis with a 15 times detector gain factor and operated in SCAN-SIM mode (SCAN:  $m/z$  35–240, SIM:  $m/z$  43, 62, 70, 71, 74, 82, 97 with a dwell time of 20 ms per ion).

The presence of DMS in ambient air at the Amazon field site was verified by comparison of retention times (7.9 min) with that of a compressed gas standard (500 ppb, Apel-Riemer) and by comparison of the mass spectra with the standard and the National Institute of Standards and Technology (NIST) mass spectral database. Quantification of ambient DMS mixing ratios was achieved by calibrating the GC-MS system with a compressed gas standard (500 parts per billion (ppb) DMS in nitrogen, Apel-Riemer, USA). Gas phase DMS mixing ratios of 0, 1.00, 1.99, 2.98, 3.97, and 4.95 ppb were generated by dynamic dilution of the DMS standard with hydrocarbon-free air. Calibration samples of 1.0 L were collected on thermal desorption tubes at  $100 \text{ mL min}^{-1}$  for 10 min. DMS calibration curves were generated for the DMS peak at 7.9 min using the peak area of the  $m/z$  62 SIM ion. A limit of detection for DMS by the analytical system was estimated to be

2.4 ppt by multiplying the calibration slope by twice the standard deviation of the  $m/z$  62 peak area of three previously desorbed sample tubes.

### 3. Results and Discussion

#### 3.1. Analytical Technique Intercomparisons

The results of the PTR-MS calibration to DMS (SIM ion  $m/z$  63, Figures S1a and S1b in the supporting information) revealed a highly linear and sensitive response. For example, the PTR-MS response to DMS was linear ( $R^2 = 0.99$ ) up to the highest mixing ratio studied (61 ppb). The calibration slope obtained using the dynamic solution injection technique (relative sensitivity:  $106,215 \text{ ppb ncps}^{-1}$ , absolute sensitivity:  $173 \text{ cps ppb}^{-1}$ ,  $1.8 \times 10^7 \text{ cps}_{21}$ ) was compared to that from dynamic dilution of the compressed gas standard (relative sensitivity:  $120,627 \text{ ppb ncps}^{-1}$ , absolute sensitivity:  $211 \text{ cps ppb}^{-1}$ ,  $2.6 \times 10^7 \text{ cps}_{21}$ ). Thus, reasonable agreement was obtained between the techniques with the relative sensitivity obtained from the DSI technique within 12% of the value obtained from the compressed gas standard. As the DSI calibration was performed during the branch emission studies in 2010 and just prior to the ambient air studies in the central Amazon, we used the PTR-MS calibration factor for DMS determined using the DSI technique to calculate all DMS mixing ratios with an estimated accuracy of 30%.

To further characterize the selectivity of the PTR-MS to DMS, we evaluated the ability of a gold-wool packed quartz glass tube to quantitatively remove DMS from a synthetic airstream. Gold wool has previously been used to selectively and quantitatively collect sulfur volatiles in air samples prior to analysis by thermal desorption, cryogenic trapping, chromatographic separation, and flame photometric detection [Andreae and Andreae, 1988]. After measuring a 1.9 ppb DMS standard by PTR-MS at  $m/z$  63, the standard was directed to flow through a gold-wool tube, which quantitatively removed the signal to background levels (Figure S2). This signal could be rapidly recovered and removed again by the removal and insertion of the gold-wool tube in the flow path. These experiments confirm that the PTR-MS signal at  $m/z$  63 can derive from the presence of DMS but do not exclude the possibility of interference from other compounds.

Given the high-moisture environments of tropical ecosystems, we assessed the potential of protonated acetaldehyde-water clusters to interfere with the PTR-MS signal at  $m/z$  63, which could lead to overestimates of DMS mixing ratios. To accomplish this, we studied the effect of introducing a high acetaldehyde mixing ratio (19 ppb) on the PTR-MS signals at  $m/z$  45 and 63 in hydrocarbon-free air humidified to a 20°C dew point (Figure S3). When acetaldehyde was introduced into zero air humidified to 20°C, a strong protonated acetaldehyde signal was detected at  $m/z$  45, but without any detectable increase in the signal at  $m/z$  63. These results demonstrate that significant protonated acetaldehyde- $\text{H}_2\text{O}$  cluster formation does not occur under our standard operating conditions. Thus, our laboratory studies suggest that the PTR-MS used in this study is highly specific and sensitive to DMS with a linear response at  $m/z$  63 from 0 to 61 ppb. Moreover, the results suggest that under the operating conditions used, stable protonated acetaldehyde- $\text{H}_2\text{O}$  cluster formation is negligible.

The calibration of the GC-MS installed in the central Amazon to DMS standard atmospheres was carried out by dynamic dilution of the compressed gas standard (SIM ion  $m/z$  62, Figures S1c and S1d). Collection and analysis of 1.0 L calibration samples of a diluted DMS standard (1.0–5.0 ppb) resulted in strong peaks with a retention time of 7.9 min with all major fragment ions present ( $m/z$  62, 61, 47, 46, 45, 35, and 27). Except for  $m/z$  27, which had elevated backgrounds due to the close proximity of acetone (7.86 min), which was also present in the standard, the ratios of ion intensities to the parent ion at  $m/z$  62 matched those from the NIST mass spectral database. In addition, the  $m/z$  62 selected ion mass chromatogram integrated peak area increased linearly with increased DMS mixing ratios up to the highest mixing ratio investigated (5.0 ppb). The results reveal that the thermal desorption GC-MS method also has high linearity ( $R^2 = 0.99$ ) and sensitivity to gas phase DMS with  $m/z$  62 peak areas of the 5.0 ppb standard reaching  $3 \times 10^7$  ion counts. Analysis of thermal desorption tubes following thermal desorption of a collected sample showed small to negligible DMS background peaks ( $m/z$  62).

#### 3.2. Branch Emissions of DMS in Relation to Light and Temperature

DMS branch emission measurements were made from seven tropical plant species within a large, enclosed rainforest mesocosm (Arizona, USA) using PTR-MS. DMS emissions from all species studied showed strong diurnal patterns, peaking between midday to early afternoon (Figures 1 and S4). Daytime branch level DMS

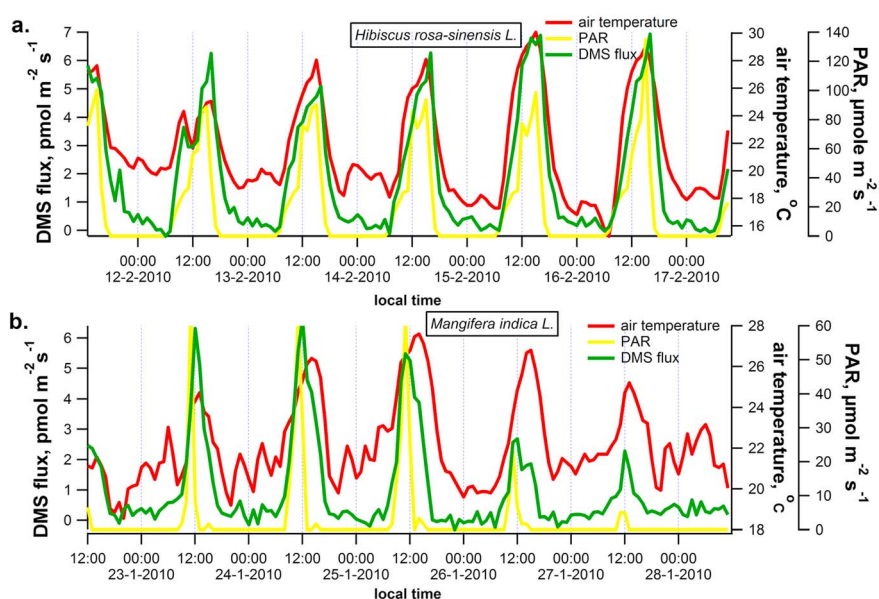


**Figure 1.** Example 5 day time series of DMS emission rates ( $\text{pmol m}^{-2} \text{s}^{-1}$ ) from isolated branches of (a) *Hibiscus rosa-sinensis L.* and (b) *Mangifera indica L.* The trees were inside a large tropical mesocosm at Biosphere 2 (Oracle, Arizona, USA) under naturally varying air temperature and photosynthetically active radiation (PAR) conditions.

emissions showed maximum values of 6, 10, 10, 6, 5, 6, and 5  $\text{pmol m}^{-2} \text{s}^{-1}$ , respectively, for *Alpinia zerumbet* (Pers.) B.L. Burt and R.M. Sm. (Zingiberaceae), *Canna indica L.* (Cannaceae), *Cissus sicyodes* (L.) Nicolson and C.E. Jarvis (Vitaceae), *Hibiscus rosa-sinensis L.* (Malvaceae), *Inga vera W.* (Fabaceae), *Mangifera indica L.* (Anacardiaceae), and *Pterocarpus indicus* Wild. (Fabaceae). The presence of DMS in branch enclosure air samples for two of the species was qualitatively verified by GC-MS (Figure S5). A clear DMS peak was present in the air exiting the branch enclosure but not the air entering the enclosure.

DMS branch emissions followed natural variations in photosynthetic active radiation (PAR) and air temperature with maximum emissions between midday to early afternoon. During the 3 month experiment, nighttime air temperature was increased in the mesocosm to prevent cold damage. However, DMS emissions were only weakly stimulated compared to emissions at the same air temperatures during the day (Figures 1 and Figure S4). Moreover, several cloudy days reduced daytime PAR fluxes and enclosure air temperature, resulting in small to negligible emissions of DMS (Figures S4c–S4e). Thus, while temperature can stimulate emissions from plants, light appears to be important. This could be mediated indirectly through light regulation of stomatal conductance or directly through incorporation of photosynthetic carbon during DMS biosynthesis. When compared with other studies on plant DMS emissions, the range of maximum DMS emissions determined from the tropical plants in this study (5–10  $\text{pmol m}^{-2} \text{s}^{-1}$ ) was found to be comparable to previously reported values. For example, in previous studies, maximum DMS emissions from *Platanus orientalis* were found to be 0.42  $\text{pmol m}^{-2} \text{s}^{-1}$  [Geng and Mu, 2006], whereas *Hibiscus sp.* was reported to emit DMS at a maximum rate of 26  $\text{pmol m}^{-2} \text{s}^{-1}$  [Yonemura et al., 2005].

The species investigated in this study represent diverse plant forms including sessile herbs (*A. zerumbet*, *C. indica*), vines (*C. cissoides*), shrubs (*H. rosa-sinensis*), and trees (*M. indica*, *P. indicus*, *I. vera*) and are all abundant genera and families with widespread tropical distributions [Smith et al., 2004]. Based on estimates of species population sizes in the Amazon Basin [Ter Steege et al., 2013], *I. vera* ranks in the 41st percentile of abundance and the genera *Inga* and *Pterocarpus* in the 99th and 94th percentiles, respectively. The families Fabaceae, Malvaceae, and Anacardiaceae ranked in the 100th, 93rd, and 80th percentiles, respectively. The abundance and diversity represented by our study species suggest the potential for widespread DMS emissions among tropical plants.

### 3.3. Soil Emissions of DMS in Relation to Soil Moisture and Temperature

A soil sample originating from an Amazonian rainforest ecosystem in Suriname was used in laboratory studies to characterize the dependency of DMS emissions on gravimetric soil moisture and soil temperature

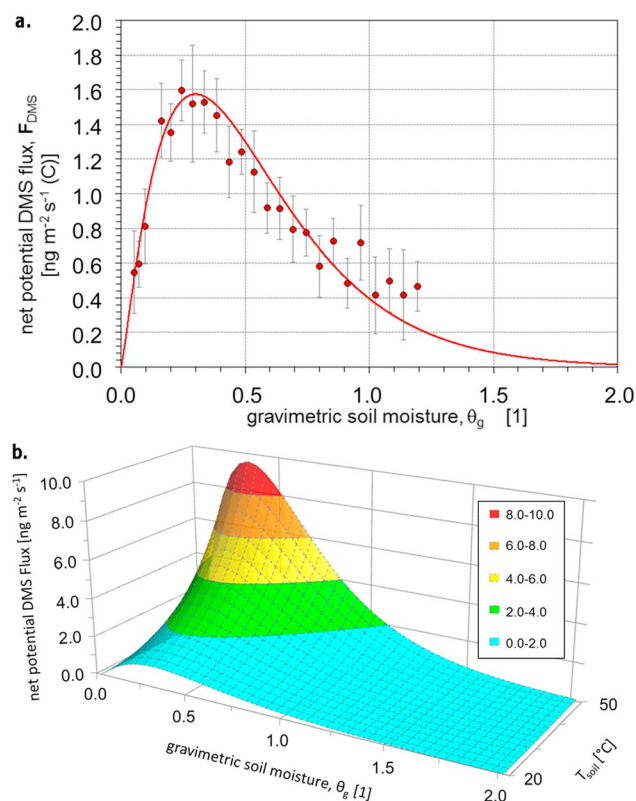


**Figure 2.** Net potential DMS flux from a soil sample collected from the Surinam Amazon as a function of (a) gravimetric soil moisture and (b) modeled gravimetric soil moisture and soil temperature by the use of a  $Q_{10}$  value of 2.06. Note that the error bars for gravimetric soil moisture are in the range of the size of the data points.

respiration rates [Kesselmeier and Hubert, 2002]. Since the incubations were performed in a dark thermostated cabinet, phototrophic processes are of minor importance. Furthermore, switching the soil temperature between 20  $^\circ\text{C}$  and 30  $^\circ\text{C}$  during drying allowed the derivation of a temperature amplification factor, the  $Q_{10}$  value, of 2.06 at  $\theta_{\text{opt}}$ , which is indicative of microbial rather than abiotic processes. Under the assumption that DMS emissions follow an enzymatically driven process, an exponential dependency to soil temperature can be applied. Figure 2 shows the model of net potential DMS flux,  $F_{\text{lab}}$ , for a soil originating from a rainforest ecosystem in Suriname, parameterized for gravimetric soil moisture and soil temperature. Prevailing field conditions for gravimetric soil moisture are likely very moist with moderate soil temperature, and therefore, the real flux under field conditions might be much lower than the maximal  $F_{\text{lab}}$  parameterized in the laboratory. Experiments with varying thicknesses of soil showed that deeper soil layers can uptake DMS and therefore reduce the release of DMS. In addition, hydrocarbon-free air was introduced into the soil enclosure which maximizes the DMS gradient between soil atmosphere and the enclosure atmosphere. Thus, our laboratory parameterization should be considered as an upper limit for  $F_{\text{lab}}$ .

### 3.4. Atmospheric Vertical Mixing Ratio Profiles of DMS Within and Above a Primary Rainforest Canopy

To gain additional insight into terrestrial DMS sources in tropical regions, we analyzed vertical ambient mixing ratio profiles of DMS within and above a central Amazon canopy on the TT34 and K34 towers. Ambient DMS mixing ratios measured by PTR-MS within the natural rainforest ecosystem were found to be in the low ppt range ( $< 160$  ppt) and highly variable with time. Figure 3 shows the mean diel patterns for six measurement periods between September 2010 and January 2011 with several important features. In most of the measurement periods, a clear enhancement of DMS mixing ratios was observed during the afternoon, with higher values within the 30 m canopy than above it. These observations are consistent with higher

and to model a net potential flux of DMS,  $F_{\text{lab}}$ . It is assumed that DMS is released by a thin layer of topsoil and therefore the soil sampling was performed for the uppermost 0.05 m. Soil from an Amazon tropical rainforest ecosystem in Suriname (5 $^\circ$ 4'34.67"N, 55 $^\circ$ 0'10.43"W) was shipped immediately after sampling to Germany for analysis (see section 1.3 in Text S1). In the laboratory, subsamples of approximately 20 g were dried out from a fully wetted condition under different soil temperatures. Figure 2 shows data from a typical incubation experiment for the DMS net release rate,  $J_{\text{DMS}}$ , starting at field capacity ( $\sim 120\%$  gravimetric soil moisture,  $\theta_g$ ) until the soil was air dried at 25  $^\circ\text{C}$  under hydrocarbon-free air. The results show that  $J_{\text{DMS}}$  follows an optimum function with  $J_{\text{DMS,max}}$  of about 19.0  $\text{pmol kg}^{-1} \text{ s}^{-1}$  at  $\theta_{\text{opt}}$  (about 30%  $\theta_g$ ). The red fit function, which was used in a previous study [Meixner, 2006] for the relationship of nitric oxide (NO) emission to gravimetric soil moisture, provides good agreement to the data. This suggests, by analogy, that an aerobic microbial process might be responsible for the release of DMS, consistent with previous findings that linked soil DMS emissions with

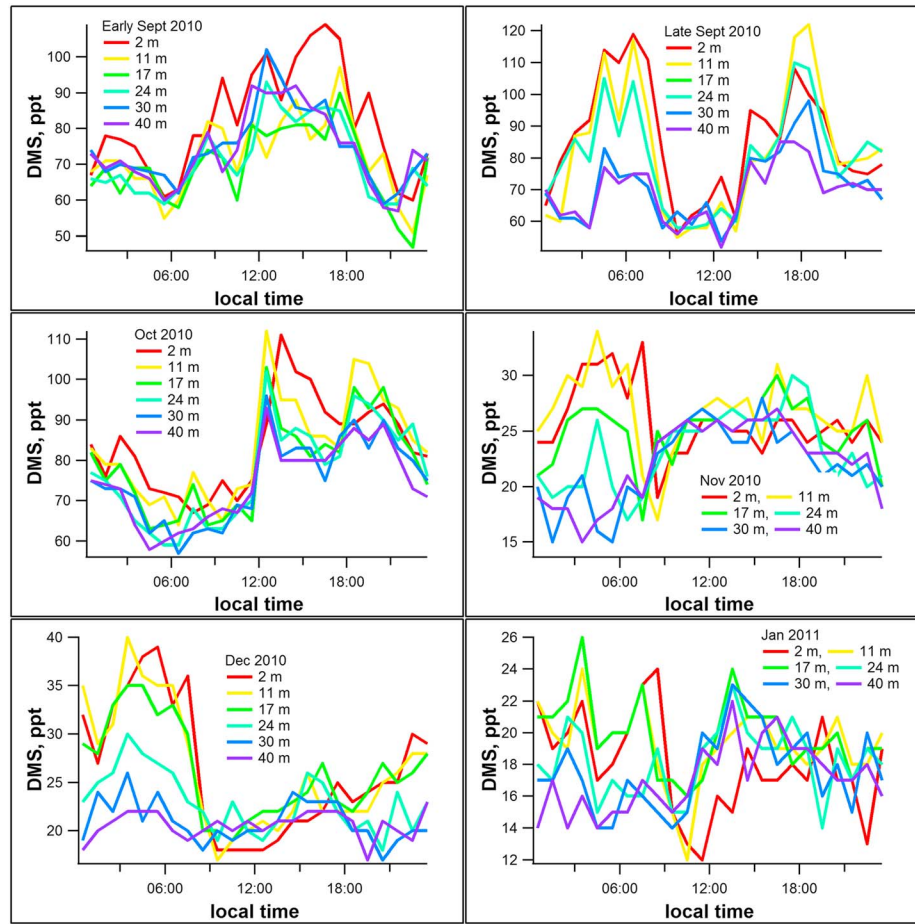


**Figure 3.** Mean diel patterns in ambient DMS mixing ratios at the TT34 site within and above the 30 m canopy between September 2010 and January 2011. Note the ambient mixing ratio enhancements within the canopy during the afternoon and evenings as well as the nocturnal buildup of ambient DMS mixing ratios within the canopy during some periods.

emission rates of DMS from vegetation and soils during the hotter periods of the day. However, during many measurement periods, DMS mixing ratios showed strong evening and nocturnal accumulations within the canopy, with mean mixing ratios up to 120 ppt. These observations could be explained by light-independent emissions of DMS at night, for example, from soils, where emissions can lead to an accumulation of DMS

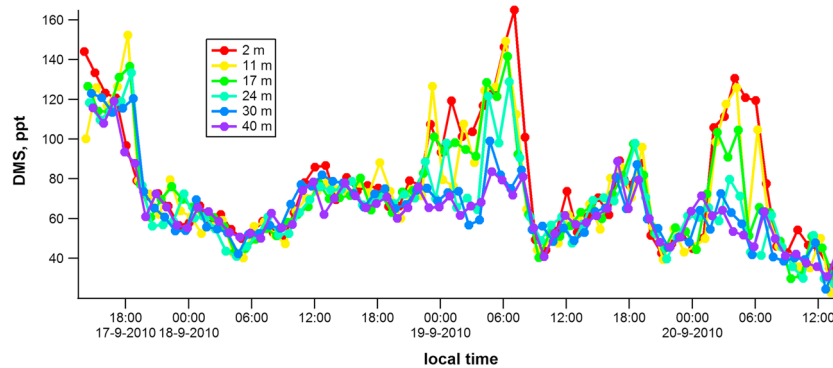


**Figure 4.** Example time series plots showing real-time ambient DMS mixing ratios within and above the canopy at the TT34 tower in central Amazon during the dry season (from 17 September to 20 September 2010). Note the buildup of DMS mixing ratios in the afternoon and during the night and early mornings just prior to sunrise within the canopy (height < 30 m).



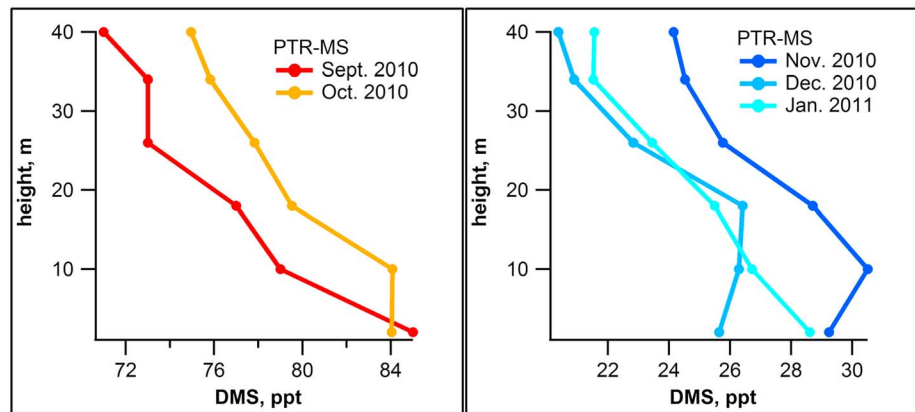


**Figure 5.** Average vertical gradient profiles of ambient DMS mixing ratios obtained by continuous PTR-MS measurements between November 2010 and January 2011 at the TT34 tower. Note the buildup of DMS mixing ratios near the ground and within the 30 m canopy.

within the canopy due to the reduced vertical mixing at night. The lowest ambient mixing ratios were observed after sunrise, possibly due to the initiation of turbulent mixing of above-canopy air, which was depleted in DMS, into the canopy. The dynamics of these events could also be observed in real time. For example, PTR-MS vertical profile measurements of DMS in September 2010 showed strong evening and nocturnal buildup of DMS mixing ratios within the canopy up to 160 ppt, with a buildup of up to 100 ppt also observed during the afternoons (Figure 4). When vertical gradients based on monthly averages were calculated, higher mixing ratios were obtained within the canopy than above (Figure 5). This suggests that the ecosystem can act as a net source of DMS to the atmosphere during both the dry and the wet seasons and during both the day and night.

To verify the presence of DMS in ambient air at the Amazon field site and to obtain quantitative comparisons with the PTR-MS measurements at the TT34 tower, we analyzed 1.0L air samples by GC-MS at the nearby K34 walkup tower at high vertical resolution. Chromatographic DMS peaks were present in thermal desorption tube samples, which were clearly higher than in the blank samples (Figure S6). Verification of the peak as DMS was based on comparisons of the retention time (7.9 min) and relative mass spectra with an authentic DMS standard (see section 2.4.1). Using thermal desorption GC-MS, highly vertically resolved DMS mixing ratios were quantified in ambient air samples collected from the K34 walkup tower between November 2013 and February 2014 (six vertical profiles were collected during the afternoon). The results show a clear buildup of

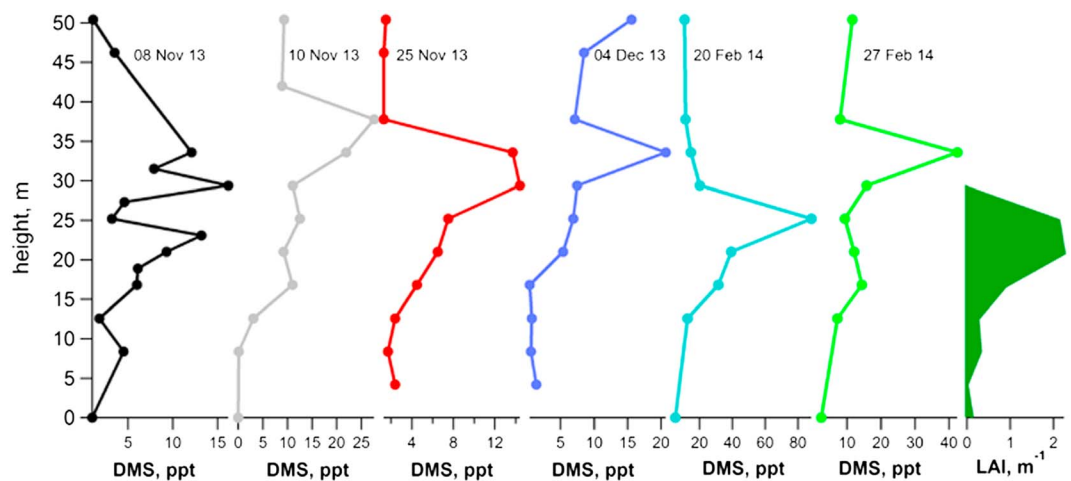


**Figure 6.** Example of high vertically resolved DMS mixing ratio measurements by GC-MS during the afternoon (13:00–15:00) on the K34 tower made between November 2013 and February 2014. Also shown are vertically resolved measurements of leaf area index (LAI). Note the buildup of DMS near the top and just above the 30 m canopy with mixing ratios up to 80 ppt.

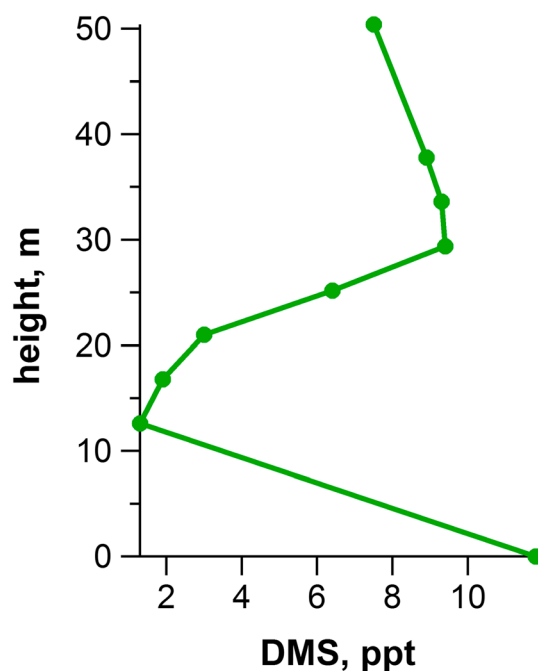


**Figure 7.** Example of high vertically resolved DMS mixing ratio measurements by GC-MS approximately 30 min following a rainstorm in the afternoon (14:06–14:55) on the K34 tower. Note that in addition to the buildup of DMS within the canopy, a buildup near the surface was observed, suggesting a potential increase in soil emissions as a result of wetting.

different years (GC-MS: 2013–2014 versus PTR-MS: 2010–2011), the results suggest limited interannual variability in the mixing ratios. GC-MS measurements showed DMS mixing ratios in November–February up to 80 ppt during the daytime while real-time PTR-MS measurements showed daytime mixing ratios in September–January that rarely exceeded 100 ppt. These results strongly suggest that the PTR-MS signal at  $m/z$  63 was largely, if not wholly, attributable to DMS. Furthermore, we compared our DMS vertical mixing ratio profiles obtained in 2010–2011 and 2013–2014 at the ZF2 reserve with those from a previous study in 1985 that measured DMS vertical mixing ratio profiles at a nearby site in the central Amazon (Reserve Ducke) using preconcentration onto gold-wool-packed tubes followed by thermal desorption, cryogenic trapping, chromatographic separation, and flame photometric detection [Andreae and Andreae, 1988]. Although a limited number of gradients were collected during the 1985 study, ambient mixing ratios were measured up to 40 ppt. Thus, despite being collected nearly three decades prior at a nearby central Amazon forest site (Reserve Ducke, Brazil), with a different analytical technique, these values fit well in the range of maximum daytime DMS mixing ratios observed in our study using GC-MS (10–80 ppt). Also consistent with our observations, DMS mixing ratios at the Ducke site in 1985 support an important role for both soil and vegetation [see Andreae and Andreae, 1988, Figure 5]; higher DMS mixing ratios were observed within the forest canopy during the morning (with highest mixing ratios near the ground) as well as midday and evening (with highest mixing ratios at the top of the canopy).

As DMS is not of anthropogenic origin and the mixing ratios above the canopy are always lower than those within the canopy, a source from vegetation and/or soil is implied by our results. Although a mixture of DMS sources from both local ecosystem emissions and long-range transport is possible, the short lifetime of DMS of 0.8–1.1 days with respect to atmospheric oxidation [Boucher *et al.*, 2003] and an estimated transport time of about 3 days to reach the central Amazon field site from the Atlantic coast by easterly winds, the majority of DMS can be assumed to derive from local emissions from vegetation and soils. However, in the Amazon rainforest there are also many ponds, wetlands, and wet areas, which could contribute to increases in the DMS mixing ratio through microbial activity [Crutzen *et al.*, 2000]. Nonetheless, our observations show that during both the day and night, DMS mixing ratios were higher within the canopy (< 30 m) than above it, suggesting

DMS mixing ratios within the top region of the 30 m canopy to levels as high as 80 ppt (Figure 6). These results suggest that during the daytime, upper canopy leaves, which are subjected to the highest light and temperature conditions, are important ecosystem sources of DMS to the atmosphere. Although most of the DMS vertical gradients showed the highest daytime mixing ratios near the top of the main canopy, a single gradient collected 30 min following a brief rainstorm in the afternoon revealed higher mixing ratios near the ground (Figure 7). As microbial respiration and DMS emissions have been shown to be stimulated following a wetting event in laboratory studies [Whelan *et al.*, 2011], and given the often strong “sulfur” smell of the petrichor just following rainstorms at the central Amazon site, the results suggest that DMS soil emissions can be enhanced during precipitation. However, additional research is needed to verify this possible phenomenon, which could lead to enhanced biota-chemistry-climate interactions in the Amazon Basin.

Given that the GC-MS measurements of DMS were conducted on a different tower than the PTR-MS measurements (due to the need for manual sample collection at each height), and during

that the ecosystem is a sustained atmospheric source of DMS not only throughout the day and night but also throughout the dry and wet seasons. Moreover, mean ambient DMS mixing ratios peaked in September during the dry season and appeared to decrease thereafter in the wet season, an expected result from the strong temperature-dependent soil and vegetation emissions observed in the laboratory and mesocosm studies. However, the source(s) of emission can only be attributed if the fluxes are calculated since concentration gradients are driven by turbulent transport, which varies throughout the canopy. High ground concentrations do not necessarily imply soil emissions because they depend on the thermodynamics and turbulent conditions in the atmospheric boundary layer. Additional research is needed to quantitatively evaluate the source(s) of DMS emissions at the ecosystem and regional scales within the Amazon forest canopies using techniques such as eddy covariance [Karl *et al.*, 2001] and inverse modeling of atmospheric concentrations based on the characterization of within-canopy turbulence [Raupach, 1989]. Thus, a quantitative assessment of the role of DMS in the Earth system requires observations of ecosystem DMS emission rates, regional extrapolations, and simulations of atmospheric chemistry and climate impacts.

Although it was impractical to obtain continuous DMS measurements using GC-MS, the real-time nature of the PTR-MS revealed enhanced temporal and vertical DMS mixing ratio dynamics that were not observed with any other PTR-MS signals measured. For example, vegetation-derived compounds such as isoprene and monoterpenes showed well-behaved patterns with maxima during the daytime within the canopy [Jardine *et al.*, 2012, 2011b], whereas compounds produced during biomass burning in the dry season showed higher mixing ratios above the canopy [Jardine *et al.*, 2011a]. Although a previous study in a Loblolly Pine forest [Berresheim and Vulcan, 1992] also found higher accumulation of DMS during the night, to our knowledge, the strong buildup of DMS mixing ratios on some nights within the Amazon forest canopy with values over 100 ppt that persisted until sunrise has not been previously observed in any terrestrial ecosystem. This accumulation is most likely the result of an active DMS source at night and a decoupled atmospheric surface layer, thus causing an increase of DMS mixing ratios because of the limited exchange with the oxidizing overlying atmosphere. Furthermore, we assume that the overall capacity of the nighttime oxidation of DMS by nitrate radicals ( $\text{NO}_3$ ) is substantially smaller than that for daytime hydroxyl radical (OH) reactions, especially if the nitrate radical mixing ratio remains low due to a sufficient sink (e.g., NO). NO emitted from soils should be of similar strength as described for the Rebio Jarú site [Gut *et al.*, 2002], indicating that  $\text{NO}_3$  should not substantially contribute to DMS oxidation at night [Chen *et al.*, 2009; Pöschl *et al.*, 2010].

#### 4. Conclusions

During significant periods of the wet season, when wet deposition is strong and biomass burning sources around the margins of the Amazon Basin are negligible, exogenous aerosol inputs to central Amazonia are small, resulting in the so-called "Green Ocean Amazon" periods [Williams *et al.*, 2002]. During these periods, aerosol particle concentrations are low, and endogenous sulfate production from DMS emissions may become important as a driver of precipitation [Barth *et al.*, 2005] through sulfuric acid-mediated NPF as well as enhancing the hygroscopicity, and therefore CCN activity, of secondary organic aerosols [Lin and Chameides, 1993; Martin *et al.*, 2010b; Roberts *et al.*, 2002; Williams *et al.*, 2001]. In this study, we demonstrate that vegetation and soils can be sources of DMS to the atmosphere in this region and confirm the presence of DMS in the central Amazon atmosphere. We present an extensive data set that suggests that the primary rainforest ecosystem is a source of DMS to the atmosphere during both the night and day, as well as throughout the year in both wet and dry seasons. Moreover, our results confirm the observations of DMS emissions from the central Amazon made in the 1980's through comparisons of measured ambient mixing ratios within and above the forest canopy. Finally, we present real-time ambient mixing ratio dynamics of DMS, showing a strong buildup of mixing ratios on some evenings and nights, possibly from light-independent soil emissions, and characterize soil emissions of DMS from an Amazonian rainforest soil as a function of temperature and soil moisture.

This confirmed that identification and characterization of the source of DMS from terrestrial ecosystems in the tropics could have important implications for climate processes in the Amazon, given that DMS oxidation can contribute to secondary sulfate and organic aerosols [Roberts *et al.*, 2002]. Through processes of NPF and enhancement of CCN activity of aerosols, a terrestrial source of DMS could therefore have implications for the hydrological cycle in the Amazonian region [Gunthe *et al.*, 2009], where a significant amount of the

precipitation is recycled via evapotranspiration leading to a potential feedback mechanism and possible terrestrial version of the CLAW hypothesis [Quinn and Bates, 2011].

## 5. Supporting Information

Details of the soil and plant enclosure systems together with PTR-MS, PTR-TOF-MS, and GC-MS methods for soil and branch emissions of DMS in the tropical rainforest mesocosm and controlled laboratory soil drying experiments, respectively, can be found in the supporting information. Additional figures can also be found in the supporting information including Figure S1: PTR-MS and GC-MS calibrations to DMS, Figure S2: PTR-MS calibration to a DMS standard without and with a gold-wool tube in line, Figure S3: analysis of potential humidity-dependent interference on the PTR-MS signal at  $m/z$  63 by a protonated acetaldehyde-water cluster, Figure S4: time series plots of DMS emission rates from isolated branches of five additional tree species growing in the large tropical rainforest mesocosm, Figure S5: GC-MS chromatogram of branch enclosure air for two tropical plant species inside the rainforest mesocosm showing the presence of DMS, and Figure S6: DMS in ambient air near the ground at the ZF2 site in the central Amazon identified by GC-MS.

## Acknowledgments

The data used in this manuscript are available for free download at [www.archive.arm.gov](http://www.archive.arm.gov). After logging in, registered users can find the data link under the "Get special data" submenu. This research was supported by the Director, Office of Science, Office of Biological and Environmental Research of the U.S. Department of Energy under contract DE-AC02-05CH11231 as part of their Terrestrial Ecosystem Science Program. Additional funding for this project came from the U.S. National Science Foundation through the AMAZON-PIRE (Partnerships for International Research and Education) award (0730305), DFG project HALOPROC 763, the NERC CLAIRE-UK project, and the German Max Planck Society. This work was also supported by Fundação de Amparo à Pesquisa do Estado de São Paulo (FAPESP-AEROCLIMA 08/58100-2). We would like to thank several individuals at the Instituto Nacional de Pesquisas da Amazônia (INPA) in Manaus, Brazil, for logistics support including Veber Moura, Roberta Pereira de Souza, and Erika Schloemp. Finally, we kindly acknowledge Cor Becker for assistance in soil sampling from Suriname.

## References

- Andreae, M. O., and T. W. Andreae (1988), The cycle of biogenic sulfur-compounds over the Amazon Basin.1 Dry season, *J. Geophys. Res.* (1984–2012), 93(D2), 1487–1497, doi:10.1029/JD093iD02p01487.
- Andreae, M., and W. Jaeschke (1992), Exchange of sulphur between biosphere and atmosphere over temperate and tropical regions, Sulphur cycling on the continents: Wetlands, Terrestrial Ecosystems, and Associated Water Bodies. SCOPE, 48, 27–61. [Available at <http://www.scopenvironment.org/downloadpubs/scope48/chapter03.html>].
- Andreae, M., H. Berresheim, H. Bingemer, D. Jacob, B. Lewis, S. M. Li, and R. W. Talbot (1990), The atmospheric sulfur cycle over the Amazon Basin: 2. Wet season, *J. Geophys. Res.* (1984–2012), 95(D10), 16,813–16,824, doi:10.1029/JD095iD10p16813.
- Banwart, W., and J. Bremner (1975), Formation of volatile sulfur compounds by microbial decomposition of sulfur-containing amino acids in soils, *Soil Biol. Biochem.*, 7(6), 359–364, doi:10.1016/0038-0717(75)90050-4.
- Barth, M., J. P. McFadden, J. Sun, C. Wiedinmyer, P. Chuang, D. Collins, R. Griffin, M. Hannigan, T. Karl, and S.-W. Kim (2005), Coupling between land ecosystems and the atmospheric hydrologic cycle through biogenic aerosol pathways, *Bull. Am. Meteorol. Soc.*, 86, 1738–1742, doi:10.1175/BAMS-86-12-1738.
- Berresheim, H., and V. D. Vulcan (1992), Vertical distributions of  $\text{CO}_2$ ,  $\text{CS}_2$ ,  $\text{DMS}$  and other sulfur-compounds in a loblolly-pine forest, *Atmos Environ Gen Top.*, 26(11), 2031–2036, doi:10.1016/0960-1686(92)90087-2.
- Betts, R., P. Cox, M. Collins, P. Harris, C. Huntingford, and C. Jones (2004), The role of ecosystem-atmosphere interactions in simulated Amazonian precipitation decrease and forest dieback under global climate warming, *Theor. Appl. Climatol.*, 78, 157–175, doi:10.1007/s00704-004-0050-y.
- Bingemer, H., M. Andreae, T. Andreae, P. Artaxo, G. Helas, D. Jacob, N. Mihalopoulos, and B. Nguyen (1992), Sulfur gases and aerosols in and above the equatorial African rain forest, *J. Geophys. Res.* (1984–2012), 97(D6), 6207–6217, doi:10.1029/91JD01112.
- Boucher, O., C. Moulin, S. Belviso, O. Aumont, L. Bopp, E. Cosme, R. V. Kuhlmann, M. Lawrence, M. Pham, and M. Reddy (2003), Dms atmospheric concentrations and sulphate aerosol indirect radiative forcing: A sensitivity study to the dms source representation and oxidation, *Atmos. Chem. Phys.*, 3(1), 49–65, doi:10.5194/acp-3-49-2003.
- Charlson, R. J., J. E. Lovelock, M. O. Andreae, and S. G. Warren (1987), Oceanic phytoplankton, atmospheric sulfur, cloud albedo and climate, *Nature*, 326(6114), 655–661, doi:10.1038/326655a0.
- Chen, Q., D. Farmer, J. Schneider, S. Zorn, C. Heald, T. Karl, A. Guenther, J. Allan, N. Robinson, and H. Coe (2009), Mass spectral characterization of submicron biogenic organic particles in the Amazon Basin, *Geophys. Res. Lett.*, 36, L20806, doi:10.1029/2009GL039880.
- Chi, X., J. Winderlich, J.-C. Mayer, A. Panov, M. Heimann, W. Birmili, J. Heintzenberg, Y. Cheng, and M. Andreae (2013), Long-term measurements of aerosol and carbon monoxide at the ZOTTO tall tower to characterize polluted and pristine air in the Siberian taiga, *Atmos. Chem. Phys.*, 13, 12,271–12,298, doi:10.5194/acp-13-12271-2013.
- Cox, P. M., P. P. Harris, C. Huntingford, R. A. Betts, M. Collins, C. D. Jones, T. E. Jupp, J. A. Marengo, and C. A. Nobre (2008), Increasing risk of Amazonian drought due to decreasing aerosol pollution, *Nature*, 453, 212–215, doi:10.1038/nature06960.
- Crutzen, P. J., et al. (2000), High spatial and temporal resolution measurements of primary organics and their oxidation products over the tropical forests of Surinam, *Atmos. Environ.*, 34(8), 1161–1165, doi:10.1016/S1352-2310(99)00482-3.
- Debruyn, W. J., E. Swartz, J. H. Hu, J. A. Shorter, P. Davidovits, D. R. Worsnop, M. S. Zahniser, and C. E. Kolb (1995), Henry's law solubilities and Setchenow coefficients for biogenic reduced sulfur species obtained from gas-liquid uptake measurements, *J. Geophys. Res.*, 100(D4), 7245–7251, doi:10.1029/95JD00217.
- Fall, R., D. L. Albritton, F. C. Fehsenfeld, W. C. Kuster, and P. D. Goldan (1988), Laboratory studies of some environmental variables controlling sulfur emissions from plants, *J. Atmos. Chem.*, 6(4), 341–362, doi:10.1007/BF00051596.
- Geng, C. M., and Y. J. Mu (2006), Carbonyl sulfide and dimethyl sulfide exchange between trees and the atmosphere, *Atmos. Environ.*, 40, 1373–1383, doi:10.1016/j.atmosenv.2005.10.023.
- Gregory, G. L., et al. (1986), Air chemistry over the tropical forest of Guyana, *J. Geophys. Res.*, 91(D8), 8603–8612, doi:10.1029/JD091iD08p08603.
- Gu, L., J. D. Fuentes, H. H. Shugart, R. M. Staebler, and T. A. Black (1999), Responses of net ecosystem exchanges of carbon dioxide to changes in cloudiness: Results from two North American deciduous forests, *J. Geophys. Res.* (1984–2012), 104(D24), 31,421–31,434, doi:10.1029/1999JD901068.
- Gunthe, S., S. King, D. Rose, Q. Chen, P. Roldin, D. Farmer, J. Jimenez, P. Artaxo, M. Andreae, and S. Martin (2009), Cloud condensation nuclei in pristine tropical rainforest air of Amazonia: Size-resolved measurements and modeling of atmospheric aerosol composition and CCN activity, *Atmos. Chem. Phys.*, 9, 7551–7575, doi:10.5194/acp-9-7551-2009.
- Gut, A., et al. (2002), Exchange fluxes of  $\text{NO}_2$  and  $\text{O}_3$  at soil and leaf surfaces in an Amazonian rain forest, *J. Geophys. Res.*, 107(D20), 8060, doi:10.1029/2001JD000654.

- Jardine, K., L. Abrell, S. A. Kurc, T. Huxman, J. Ortega, and A. Guenther (2010a), Volatile organic compound emissions from *Larrea tridentata* (creosotebush), *Atmos. Chem. Phys.*, *10*, 12,191–12,206, doi:10.5194/acp-10-12191-2010.
- Jardine, K., W. Henderson, T. Huxman, and L. Abrell (2010b), Dynamic Solution Injection: A new method for preparing pptv & ppbv standard atmospheres of volatile organic compounds, *Atmos. Meas. Tech.*, *3*, 1569–1576, doi:10.5194/amt-3-1569-2010.
- Jardine, K., et al. (2011a), Ecosystem-scale compensation points of formic and acetic acid in the central amazon, *Biogeosciences*, *8*, 3709–3720, doi:10.5194/bg-8-3709-2011.
- Jardine, K., L. Abrell, A. M. Yanez Serrano, A. Arneht, F. Y. Ishida, T. Huxman, S. Saleska, A. Jardine, T. Karl, and P. Artaxo (2011b), Within-canopy sesquiterpene ozonolysis in Amazonia, *J. Geophys. Res.*, *116*, D19301, doi:10.1029/2011JD016243.
- Jardine, K., et al. (2012), Within-plant isoprene oxidation confirmed by direct emissions of oxidation products methyl vinyl ketone and methacrolein, *Global Change Biol.*, *18*, 973–984, doi:10.1111/j.1365-2486.2011.02610.x.
- Kanda, K.-I., and H. Tsuruta (1995), Emissions of sulfur gases from various types of terrestrial higher plants, *Soil Sci. Plant Nutr.*, *41*(2), 321–328, doi:10.1080/00380768.1995.10419589.
- Karl, T., A. Guenther, C. Lindinger, A. Jordan, R. Fall, and W. Lindinger (2001), Eddy covariance measurements of oxygenated volatile organic compound fluxes from crop harvesting using a redesigned proton-transfer-reaction mass spectrometer, *J. Geophys. Res.*, *106*(D20), 24,157–24,167, doi:10.1029/2000JD000112.
- Karl, T., A. Guenther, A. Turnipseed, G. Tyndall, P. Artaxo, and S. Martin (2009), Rapid formation of isoprene photo-oxidation products observed in Amazonia, *Atmos. Chem. Phys.*, *9*, 7753–7767, doi:10.5194/acp-9-7753-2009.
- Kesselmeier, J., and A. Hubert (2002), Exchange of reduced volatile sulfur compounds between leaf litter and the atmosphere, *Atmos. Environ.*, *36*(29), 4679–4686, doi:10.1016/s1352-2310(02)00413-2.
- Kesselmeier, J., F. X. Meixner, U. Hofmann, A.-L. Ajavon, S. Leimbach, and M. O. Andreae (1993), Reduced sulfur compound exchange between the atmosphere and tropical tree species in southern Cameroon, *Biogeochemistry*, *23*(1), 23–45, doi:10.1007/BF00002921.
- Kettle, A., and M. Andreae (2000), Flux of dimethylsulfide from the oceans: A comparison of updated data sets and flux models, *J. Geophys. Res.* (1984–2012), *105*(D22), 26,793–26,808, doi:10.1029/2000JD900252.
- Kulmala, M., V. M. Kerminen, T. Anttila, A. Laaksonen, and C. D. O’ Dowd (2004), Organic aerosol formation via sulphate cluster activation, *J. Geophys. Res.*, *109*, D04205, doi:10.1029/2003JD003961.
- Lamb, B., H. Westberg, G. Allwine, L. Bamesberger, and A. Guenther (1987), Measurement of biogenic sulfur emissions from soils and vegetation: Application of dynamic enclosure methods with Natusch filter and GC/FPD analysis, *J. Atmos. Chem.*, *5*(4), 469–491, doi:10.1007/BF00113906.
- Lin, X., and W. Chameides (1993), CCN formation from DMS oxidation without SO<sub>2</sub> acting as an intermediate, *Geophys. Res. Lett.*, *20*(7), 579–582, doi:10.1029/93GL00805.
- Lovelock, J. E., R. Maggs, and R. Rasmussen (1972), Atmospheric dimethyl sulphide and the natural sulphur cycle, *Nature*, *237*, 452–453, doi:10.1038/237452a0.
- Malhi, Y., and J. Grace (2000), Tropical forests and atmospheric carbon dioxide, *Trends Ecol. Evol.*, *15*(8), 332–337, doi:10.1016/S0169-5347(00)01906-6.
- Martin, S. T., et al. (2010a), An overview of the Amazonian Aerosol Characterization Experiment 2008 (amaze-08), *Atmos. Chem. Phys.*, *10*, 11,415–11,438, doi:10.5194/acp-10-11415-2010.
- Martin, S. T., M. O. Andreae, P. Artaxo, D. Baumgardner, Q. Chen, A. H. Goldstein, A. Guenther, C. L. Heald, O. L. Mayol-Bracero, and P. H. McMurry (2010b), Sources and properties of Amazonian aerosol particles, *Rev. Geophys.*, *48*, doi:10.1029/2008RG000280.
- Meixner, F. (2006), Biogenic emissions of nitric oxide and nitrous oxide from arid and semi-arid land, *Dryland ecohydrology*, 233–255, doi:10.1007/1-4020-4260-4\_14.
- Myers, N. (1991), Tropical forests: Present status and future outlook, *Clim. Change*, *19*(1–2), 3–32, doi:10.1007/BF00142209.
- Phillips, O. L., L. E. Aragão, S. L. Lewis, J. B. Fisher, J. Lloyd, G. López-González, Y. Malhi, A. Monteagudo, J. Peacock, and C. A. Quesada (2009), Drought sensitivity of the Amazon rainforest, *Science*, *323*, 1344–1347, doi:10.1126/science.1164033.
- Pöschl, U., S. Martin, B. Sinha, Q. Chen, S. Gunthe, J. Huffman, S. Borrmann, D. Farmer, R. Garland, and G. Helas (2010), Rainforest aerosols as biogenic nuclei of clouds and precipitation in the Amazon, *Science*, *329*, 1513–1516, doi:10.1126/science.1191056.
- Quinn, P. K., and T. S. Bates (2011), The case against climate regulation via oceanic phytoplankton sulphur emissions, *Nature*, *480*, 51–56, doi:10.1038/Nature10580.
- Raupach, M. R. (1989), Applying Lagrangian fluid-mechanics to infer scalar source distributions from concentration profiles in plant canopies, *Agr Forest Meteorol.*, *47*(2–4), 85–108, doi:10.1016/0168-1923(89)90089-0.
- Roberts, G. C., P. Artaxo, J. Zhou, E. Swietlicki, and M. O. Andreae (2002), Sensitivity of CCN spectra on chemical and physical properties of aerosol: A case study from the Amazon Basin, *J. Geophys. Res.* (1984–2012), *107*(D20), LBA 37-1–LBA 37-18, doi:10.1029/2001JD000583.
- Sipilä, M., T. Berndt, T. Petäjä, D. Brus, J. Vanhanen, F. Stratmann, J. Patokoski, R. L. Mauldin, A.-P. Hyvärinen, and H. Lihavainen (2010), The role of sulfuric acid in atmospheric nucleation, *Science*, *327*, 1243–1246, doi:10.1126/science.1180315.
- Smith, N., S. A. Mori, A. Henderson, D. W. Stevenson, and S. V. Heald (2004), *Flowering Plants of the Neotropics*, Princeton Univ. Press, Princeton, N. J.
- Staubes, R., H. W. Georgii, and G. Ockelmann (1989), Flux of COS, DMS and CS<sub>2</sub> from various soils in Germany, *Tellus B.*, *41*(3), 305–313, doi:10.1111/j.1600-0889.1989.tb00309.x.
- Ter Steege, H., N. C. Pitman, D. Sabatier, C. Baraloto, R. P. Salomão, J. E. Guevara, O. L. Phillips, C. V. Castilho, W. E. Magnusson, and J.-F. Molino (2013), Hyperdominance in the Amazonian tree flora, *Science*, *342*(6156), 1243092, doi:10.1126/science.1243092.
- Thomas, M. A., P. Suntharalingam, L. Pozzoli, S. Rast, A. Devasthale, S. Kloster, J. Feichter, and T. M. Lenton (2010), Quantification of DMS aerosol-cloud-climate interactions using the ECHAM5-HAMMOZ model in a current climate scenario, *Atmos. Chem. Phys.*, *10*(15), 7425–7438, doi:10.5194/acp-10-7425-2010.
- Watts, S. F. (2000), The mass budgets of carbonyl sulfide, dimethyl sulfide, carbon disulfide and hydrogen sulfide, *Atmos. Environ.*, *34*(5), 761–779, doi:10.1016/S1352-2310(99)00342-8.
- Whelan, M., M. H. Khan, K. Barnash, J. Vollering, R. Rhew (2011), DMS pulse and COS valley: The effect of simulated rainfall on sulfur gas exchange in dry soils of uncultivated marine terraces, In American Geophysical Union, Fall Meeting 2011, abstract #B11A-0463, San Francisco, Calif.
- Williams, E., et al. (2002), Contrasting convective regimes over the Amazon: Implications for cloud electrification, *J. Geophys. Res.* (1984–2012), *107*(D20), LBA 50-1–LBA 50-19, doi:10.1029/2001JD000380.
- Williams, J., U. Poschl, P. J. Crutzen, A. Hansel, R. Holzinger, C. Warneke, W. Lindinger, and J. Lelieveld (2001), An atmospheric chemistry interpretation of mass scans obtained from a proton transfer mass spectrometer flown over the tropical rainforest of Surinam, *J. Atmos. Chem.*, *38*(2), 133–166, doi:10.1023/A:1006322701523.
- Yang, Z., K. Kanda, H. Tsuruta, and K. Minami (1996), Measurement of biogenic sulfur gases emission from some Chinese and Japanese soils, *Atmos. Environ.*, *30*(13), 2399–2405, doi:10.1016/1352-2310(95)00247-2.

- Yonemura, S., L. Sandoval-Soto, J. Kesselmeier, U. Kuhn, M. Von Hobe, D. Yakir, and S. Kawashima (2005), Uptake of carbonyl sulfide (COS) and emission of dimethyl sulfide (DMS) by plants, *Phyton-Annales Rei Botanicae*, *45*, 17–24, doi:10.5194/bg-9-2935-2012.
- Zhang, J., L. Wang, and Z. Yang (2004), Emission of biogenic sulfur gases from the microbial decomposition of cystine in Chinese rice paddy soils, *Bull. Environ. Contam. Toxicol.*, *72*, 850–857, doi:10.1007/s00128-004-0322-3.
- Zhigang, Y., W. Xinming, S. Guoying, and F. Jiamo (2008), Exchange of carbonyl sulfide (OCS) and dimethyl sulfide (DMS) between rice paddy fields and the atmosphere in subtropical China, *Agric., Ecosyst. Environ.*, *123*, 116–124, doi:10.1016/j.agee.2007.05.011.
- Zhigang, Y., W. Xinming, O. Mingan, Z. Deqiang, and Z. Guoyi (2010), Air-soil exchange of dimethyl sulfide, carbon disulfide, and dimethyl disulfide in three subtropical forests in south China, *J. Geophys. Res.* (1984–2012), *115*, D18302, doi:10.1029/2010JD014130.